



3 PRELIMINARY RESULTS ON THE LUNAR GRAVITATIONAL FIELD FROM
ANALYSIS OF LONG-PERIOD AND SECULAR EFFECTS ON LUNAR ORBITER I

W. Thomas Blackshear, Harold R. Compton, and James R. Schiess

NASA Langley Research Center
Langley Station, Hampton, Va.

Presented at NASA Seminar on Guidance Theory and Trajectory Analysis

GPO PRICE \$ _____

CFSTI PRICE(S) \$ _____

Hard copy (HC) _____

Microfiche (MF) _____

ff 653 July 65

FACILITY FORM 602	N 68-27572	(THRU)
	(ACCESSION NUMBER)	
	25	(CODE)
	38	(CATEGORY)
	(PAGES)	
	TIN-60127	
	(NASA CR OR TMX OR AD NUMBER)	

Electronics Research Center
Cambridge, Massachusetts
May 31 - June 1, 1967 214

PRELIMINARY RESULTS ON THE LUNAR GRAVITATIONAL FIELD FROM
ANALYSIS OF LONG-PERIOD AND SECULAR EFFECTS ON LUNAR ORBITER I

W. Thomas Blackshear, Harold R. Compton, and James R. Schiess
NASA - Langley Research Center, Hampton, Virginia

ABSTRACT

The Doppler tracking data from the first lunar satellite established by the United States, Lunar Orbiter I, have been used to determine the long-period and secular variations in the Keplerian orbital elements. These variations have been analyzed to determine a preliminary set of coefficients in the expansion of the lunar gravitational field in terms of spherical harmonics.

The methods used to determine the long-period and secular variations in the orbital elements and to reduce these variations to determine the gravitational field coefficients are presented. Also presented in this paper are time histories of the orbital elements, Doppler residual plots, curves showing the fits to the mean orbital elements and a preliminary estimate of a set of gravitational field coefficients.

INTRODUCTION

The objective of this investigation is the determination of a mathematical model for the gravitational field of the moon. The Lunar Orbiter Project offers a unique opportunity to accomplish this objective, because

for the first time almost continuous observations of a close lunar satellite can be made. The perturbations in the orbit of such satellites are almost entirely due to the combined gravitational fields of the moon, earth and sun because of the absence of any appreciable atmosphere. To be more specific, the object is to determine a finite number of the coefficients $C_{n,m}$ and $S_{n,m}$ in the infinite series expansion of the lunar gravitational potential function in spherical harmonics

$$U = \frac{\mu}{r} \left[1 + \sum_{n=2}^{\infty} \sum_{m=0}^{\infty} \left(\frac{R}{r} \right)^n P_{n,m} (\sin \phi) (C_{n,m} \cos m\lambda + S_{n,m} \sin m\lambda) \right] \quad (1)$$

where μ is the product of the gravitational constant and the mass of the moon, R is the mean radius of the moon, r is the radial distance from the center of mass of the moon, $P_{n,m}$ are the associated Legendre polynomials, and ϕ and λ are the selenographic latitude and longitude respectively.

In order to accomplish the objective stated above a method was used which can be referred to as a "long-period" method. The mean orbital elements are determined daily from fits to short arcs of tracking data. The long-period and secular variations of these mean elements are then analyzed to determine the lunar gravitational field coefficients. Both the determination of the mean element sets and the analysis of the variations make use of the procedures of iterative differential corrections, weighted

least squares, and numerical integration of the equations of motion of the lunar spacecraft. A more detailed description of these procedures is given in a subsequent discussion.

DOPPLER DATA DESCRIPTION

The data used to determine the mean elements were coherent two-way Doppler frequency obtained from radar tracking of the Lunar Orbiter I spacecraft. The geometry of the earth, moon, tracking station and spacecraft is illustrated in figure 1. The observation is two-way in that a radio signal is transmitted from earth to the spacecraft and retransmitted to earth. The frequency received at the tracking station is differenced with the transmitted frequency to obtain the Doppler shift due to the relative velocity between spacecraft and tracking station. The Doppler data is coherent in that the transmitter frequency and the receiver comparison frequency are generated by the same oscillator, as indicated by the hardline connection between stations. For the data used in this investigation these are physically the same station, having a different position at signal transmission and receipt due primarily to earth rotation. It is evident that the Doppler shift depends on spacecraft state (position and velocity) and hence this dependence can be used to solve for state from the Doppler observations.

PROCEDURE FOR DATA REDUCTION

As stated earlier a differential correction, weighted least squares technique is used as the basic procedure in processing both Doppler data and mean element sets.

$$f_{\text{obs}}(t) = F(\text{real world}, \bar{x})$$

$$f_{\text{comp}}(t) = F(\text{eqns. of motion, parameter estimates } \bar{x}_0)$$

$$\Delta f(t) = f_{\text{comp}}(t) - f_{\text{obs}}(t)$$

$$= \left(\frac{\partial f}{\partial \bar{x}} \right)_t \left(\frac{\partial \bar{x}}{\partial \bar{x}_0} \right) \Delta \bar{x}_0 + \epsilon = A \Delta \bar{x}_0 + \epsilon$$

$$\Delta \bar{x}_0 = (A^T W A)^{-1} A^T W \Delta f$$

$$(A^T W A)^{-1} = \begin{pmatrix} \sigma_{x_1}^2 & \rho_{x_1 x_2} \sigma_{x_1} \sigma_{x_2} & \dots \\ \cdot & \sigma_{x_2}^2 & \cdot \\ \cdot & \cdot & \cdot \\ \cdot & \cdot & \cdot & \sigma_{x_n}^2 \end{pmatrix}$$

First an observable, f , is measured at some time t . The observable is a function of the true conditions, i.e. station locations, spacecraft state,

gravitational field, etc. The true values of these parameters are represented by the vector \bar{x} . Second a value of the observable is computed at the time corresponding to the observation. This computation is based on a mathematical description of the true conditions and estimates \bar{x}_0 of the values of the parameters in \bar{x} . The functional relationship between data and parameters is linearized by relating incremental differences between the computed and measured values of the observable, called residuals, to incremental differences in the values of the parameter set.

$\left(\frac{\partial f}{\partial \bar{x}}\right)_t$ is the geometric part of the total differential and $\left(\frac{\partial \bar{x}_t}{\partial \bar{x}_0}\right)$ is

the dynamic part, bringing in the effect of the force field. The parameter

ϵ is an error vector arising from such sources as measurement error, computational error, incomplete mathematical model and non-linearities in the relationship. This equation is solved to obtain an estimate of the error in a subset of the initial parameter values which minimizes the weighted sum-of-squares of the residuals, $\epsilon^T W \epsilon$, where W is a weighting matrix. If the error vector ϵ is a sample from a random distribution with zero mean then the matrix $(A^T W A)^{-1}$ is the covariance matrix of the parameter set \bar{x} ; i.e. it yields the variances on each parameter and the linear correlations between parameters. The conditions which must be fulfilled for $(A^T W A)^{-1}$ to be a covariance matrix have seldom been met, thus this matrix is used as a measure of sensitivity of the data to the parameters in the solution set.

REDUCTION OF DOPPLER DATA TO DETERMINE MEAN ELEMENTS

With the use of Doppler observations at specified intervals over some extended time period, a two step data reduction procedure is performed to determine the mean orbital elements during these specified intervals of time. The first step is to process Doppler observations spanning about one day to determine the spacecraft state at a particular time. Next, based on this estimate of state the equations of motion are numerically integrated over one orbital period. The osculating states thus generated are averaged to obtain a smoothed or mean value of the orbital elements for that particular orbit. This process is repeated for each available day of tracking data.

The specific representation of the spacecraft orientation that is determined is illustrated in figure 2. The coordinate system is inertial, chosen to coincide with the selenographic system at some instant in time; i.e. the x-y plane is the lunar equator, the x-axis coincides with the mean earth-moon line through Sinus Medii. The conventional Kepler orbital elements are referenced to this system: longitude of ascending node, Ω , is measured from the x axis in the x-y plane; argument of pericenter, ω , is measured in the orbital plane from the ascending node; inclination, i , is measured with respect to the x-y plane; true anomaly, v , is measured from pericenter to the spacecraft; and mean anomaly, M , is measured from pericenter. The semi-major axis and eccentricity complete the description of the orbit.

In the long period procedure it is only required to obtain spacecraft state by processing the Doppler data. However there is a question of what if anything should be included in the solution along with state. It was assumed that all significant physical quantities, exclusive of the moon's gravitational field, were sufficiently well determined to allow fixing their values. Thus the solution set was restricted to contain spacecraft state and lunar harmonic coefficients. The question then remained of which coefficients to include.

In order to provide an efficient method for processing many one day blocks of Doppler data, it was decided that a fixed number of harmonic coefficients would be included in the solution. By fixed it is meant that the degree and order of the coefficients in this set would remain the same for each block of data to be processed but not necessarily the values of the coefficients. The selection of the coefficients to be included in the solution was made after analyzing the results of fitting several orbits of doppler data with solution sets containing spacecraft state and various combinations of harmonic coefficients. Doppler residual plots corresponding to some of these solutions are shown in figure 3. The top curve is for a state only solution. The center curve is for state plus the five harmonic coefficients of degree two. The lower curve is for state plus 12 harmonic coefficients, five of degree two and seven of degree three. All these plots exhibit the results of an incomplete mathematical model, however the lower curve represents an

order of magnitude improvement in the residuals. The inclusion of additional harmonic coefficients failed to significantly improve the situation and eventually led to a problem of numerical ill-conditioning. Thus the solution set of state plus the twelve harmonic coefficients through degree and order three was selected as being the most efficient, with respect to computer time, while affording sufficient degrees of freedom to yield an acceptable fit to the Doppler data. The largest residuals on these curves occur in the region of pericenter. It seems most probable at the present time to infer that the periodic behavior in the residuals is due to an insufficient number of terms being included in the series representation of the lunar gravitational field.

It follows from the above discussion that it is possible to determine the lunar gravitational field directly from processing the Doppler data. This direct approach is currently being conducted at Langley, see reference 1, in addition to the indirect or long-period method presented in this paper.

Having selected the solution set, the reduction of doppler data yields an osculating value of state at some specific epoch. Since the long-period theory is based on mean rather than osculating state it is desirable to smooth this osculating state at epoch by integrating the equations of motion over one orbital period, storing osculating state at five minute intervals and averaging these states. The average state,

time tagged at the mid-point of the integration interval, is taken as the mean elements in the long-period theory. That this hypothesis is only approximately true is illustrated in figure 4 which shows variations in the orbital elements over one orbital period. The solid line on each plot represents the average value. Each plot begins and ends at apocenter, with the major variation occurring in the region of pericenter. The major portion of this variation is probably pseudo physical in the sense that there theoretically exists a gravitational field which would produce such a variation, namely the one used to generate these plots. However, this gravitational field yielded a relatively poor fit to the Doppler data in the region of pericenter and hence is less representative of physical reality in that region.

The top curve in figure 4 is for the semi-major axis and it essentially repeats after one orbit which is consistent with long-period theory which asserts that there is no long-period variation in the semi-major axis; however, in this analysis the short-period variation appears to have introduced a bias into the determination of the mean element as will be shown later. In the lower two curves for eccentricity and inclination, the long-period variation is becoming apparent after one orbital period and again the mean element determination has been biased by the short period variation. However this bias can be tolerated if it proves to be reasonably random from day to day and if a sufficient number of mean element sets can be produced. Whether this is the situation might be inferred from figure 5.

The points on figure 5a represent mean element determinations. The solid curve on the top plot shows the variation in eccentricity due to the combined earth-sun effect with the earth effect being dominant. The difference between the solid curve and the data points represents the effect of the non-central gravitational field of the moon. The large variation in eccentricity obscures the noise on these determinations, however on the lower plot for the semi-major axis, which is theoretically constant, the noise is obvious, spanning a region of about one kilometer.

Figure 5b is a continuation of the mean element plots. The solid curve on the upper plot again represents the combined earth-sun effect on the longitude of ascending node. The data noise is again more evident on the lower plot for inclination. The increase in the noise level following day 20 is due to a decrease in tracking coverage.

REDUCTION OF MEAN ORBITAL ELEMENTS TO DETERMINE LUNAR GRAVITATIONAL FIELD

The determination of the gravitational field from the long-period and secular variations in the mean orbital elements requires a description of this field in terms of these elements. Such a description is given by a transformation of the general term of the series in equation (1) to a function of the Keplerian orbital elements.

$$U_{n,m} = \frac{\mu R^n}{a^{n+1}} \sum_{p=0}^n F_{nmp}(i) \sum_{q=-\infty}^{\infty} G_{npq}(e) S_{nmpq}(\omega, M, \Omega, \theta) \quad (2)$$

$$\begin{aligned}
 S_{nmpq} = & \begin{cases} C_{n,m} & n-m \text{ even} \\ -S_{n,m} & n-m \text{ odd} \end{cases} \cos \left[(n - 2p) \omega + (n - 2p + q) M + m(\Omega - \theta) \right] \\
 + & \begin{cases} S_{n,m} & n-m \text{ even} \\ C_{n,m} & n-m \text{ odd} \end{cases} \sin \left[(n - 2p) \omega + (n - 2p + q) M + m(\Omega - \theta) \right]
 \end{aligned} \tag{3}$$

A complete description of all the terms in this formulation of the potential function is given in reference 2. The term S_{nmpq} is written out to show that short-period variations arise from a trigonometric function which includes mean anomaly as one of its arguments. In long-period theory the coefficient of mean anomaly is assumed to be zero. The remaining functions in the general term $U_{n,m}$ (i.e. $F_{nmp}(i)$ and $G_{nmp}(e)$) become slowly varying functions of time. This theoretical assumption has been approximated by averaging the elements over 360° in mean anomaly to yield a corresponding long-period variation.

Processing the variation in these mean elements yields the set of lunar harmonic coefficients shown on table 1. These are preliminary values for the coefficients and, although they represent a good fit to Lunar Orbiter I data, they will probably be modified when data from later Lunar Orbiter missions are included. The quality of the data fit provided by these coefficients is shown on figure 6a. There is good agreement on

the eccentricity and semi-major axis plots except in the region of very high noise level from day 40 on.

Figure 6b shows the corresponding fit for longitude of ascending node and inclination. Because of the small scale on the inclination plot it can be seen that the variations produced by this gravitational field are more oscillatory than is preferred based on visual inspection of the data. This oscillation could be smoothed by more appropriate selection of data weights, which for this fit were determined empirically. However it is believed that the same smoothing can be accomplished more efficiently by including data from later Lunar Orbiter missions and efforts are now being directed to this end.

The real test of the validity of a gravitational field model is its ability to predict behavior for all orbital situations. Lunar Orbiter Missions II and III permit a partial check of the gravitational field that has been presented. This is illustrated on figure 7 which shows radius of pericenter predictions for Lunar Orbiters I, II and III. This parameter is of interest for satellite lifetime predictions. The top curve represents a fit rather than a prediction since the points on this plot are derived from the mean elements determined by Langley post-flight analysis. The lower two plots represent true predictions. The points on these two plots were generated from osculating values of state obtained by the Boeing Company during real time mission control. The shape of the orbits for Missions II and III are basically the same as for Mission I, the more

pronounced difference being in inclination. It is seen that with the five degree inclination change between Missions I and II the radius of pericenter prediction for Lunar Orbiter II is off by about ten kilometers after 35 days. With the nine degree inclination difference between Missions I and III the radius of pericenter prediction for Lunar Orbiter III is off by about 10 kilometers after 25 days. Although the results presented here represent a considerable increase in knowledge relative to pre-Lunar Orbiter I knowledge of the lunar gravitational field, there is additional information to be gained from these latter missions. Thus it follows that the primary effort now is the inclusion of this data into the gravitational field determination procedure.

CONCLUDING REMARKS

A preliminary set of lunar gravitational coefficients has been presented, with the qualification that the values may be subject to modification as more data from future Lunar Orbiters are analyzed. One reason for expecting these modifications is the inability of the given set of coefficients to predict pericenter radius variations of Lunar Orbiters II and III very accurately. It is expected that tracking data from future Lunar Orbiters having significantly different orbital parameters, in particular the inclinations, can be used to reduce correlations between certain of the coefficients and therefore provide a better estimate of these coefficients. Also with the use of more tracking data it may be

- 14 -

possible to solve for a larger number of coefficients. Work is currently underway at the Langley Research Center to include Lunar Orbiter II tracking data in the long period process for the determination of the lunar gravity field.

REFERENCES

1. Michael, William H., Jr.; Tolson, Robert H.; and Gapecynski, John P.: Preliminary Results on the Gravitational Field of the Moon from Analysis of Lunar Orbiter Tracking Data. Presented at the American Geophysical Union Annual Meeting, Washington, D. C., April 17-20, 1967.
2. Kaula, W. M.: Analysis of Gravitational and Geometric Aspects of Geodetic Utilization of Satellites. Geophysical Journal of Royal Astronomical Society, vol. 5, no. 2, July 1961, pp. 104-133.

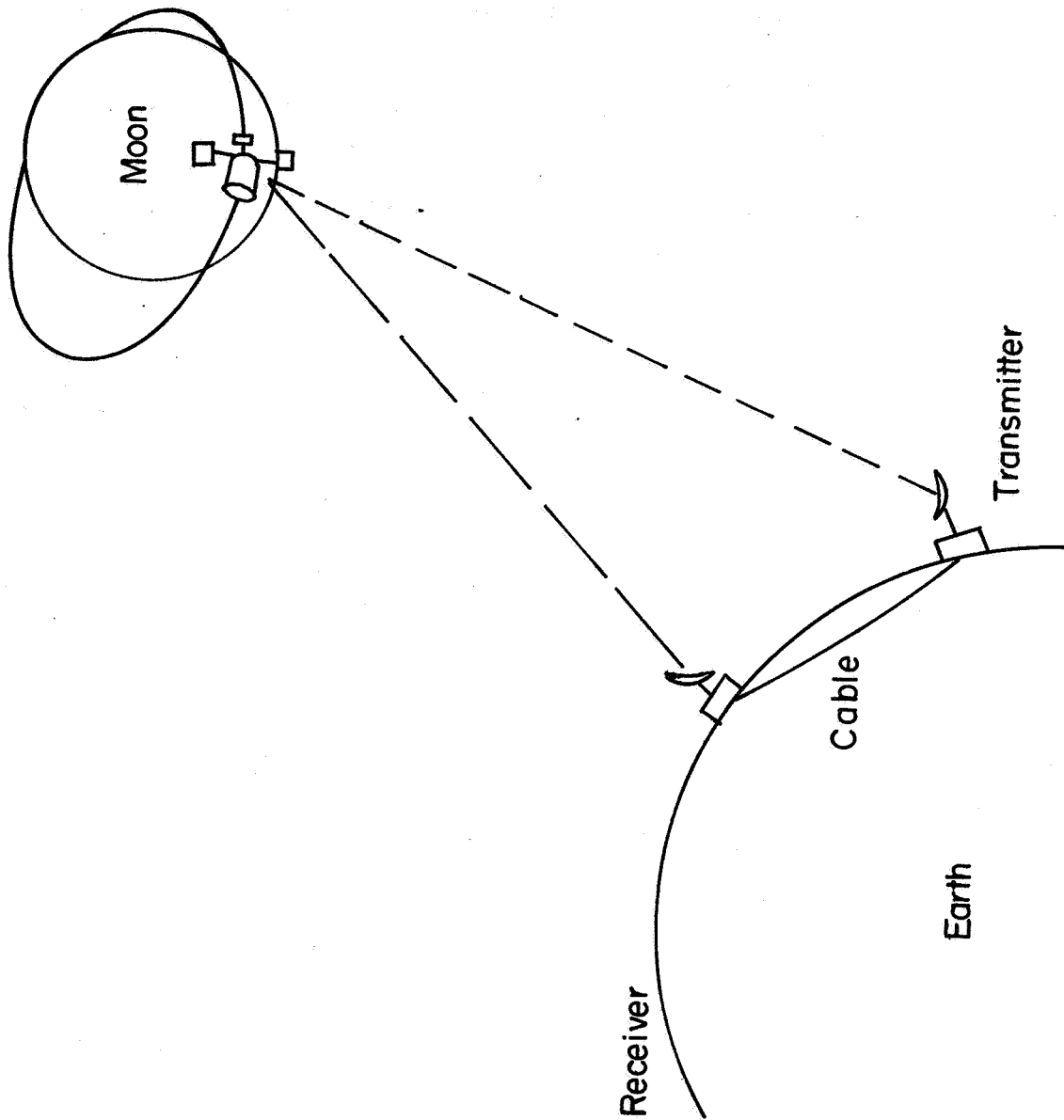


Figure 1.- Tracking geometry.

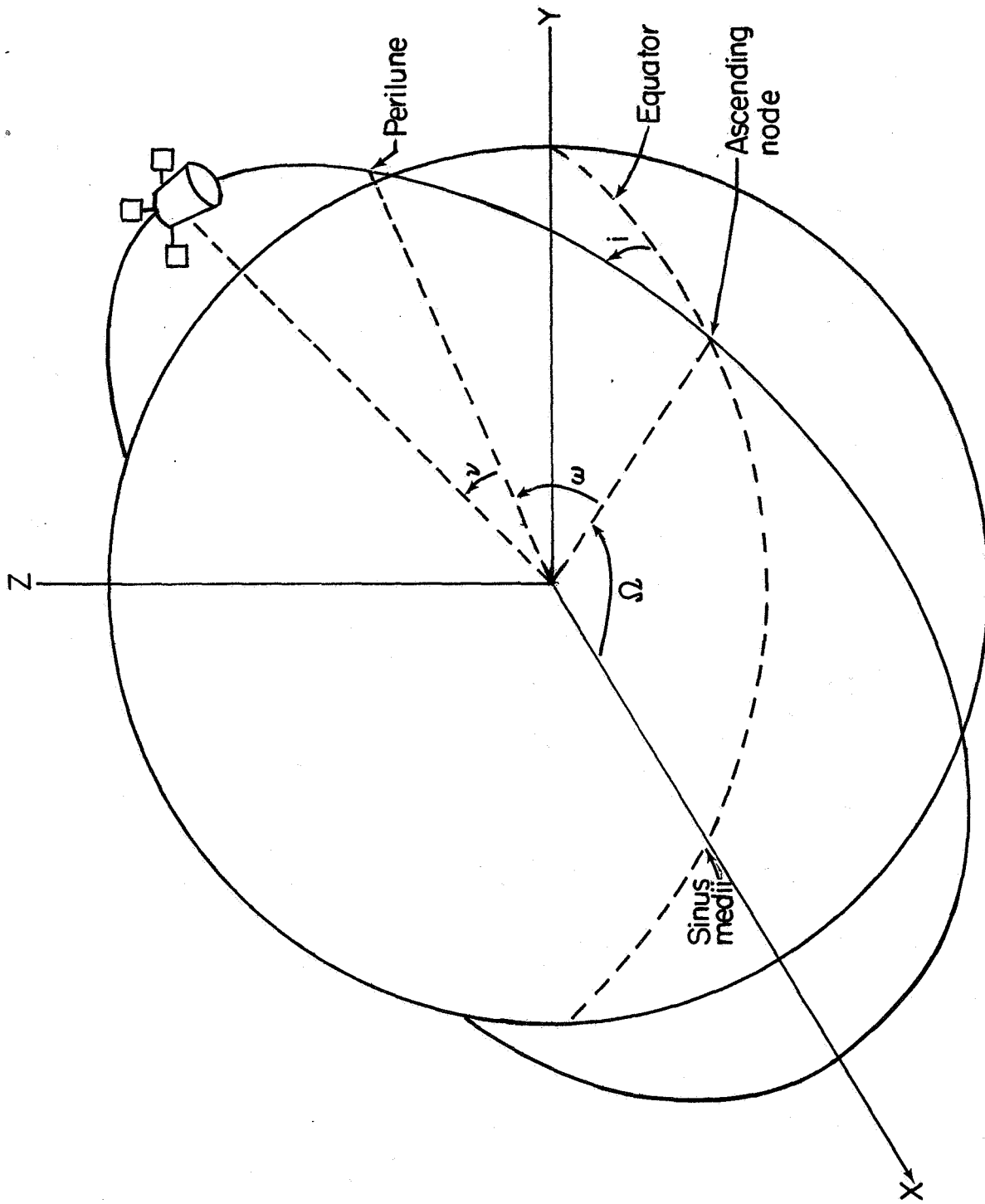


Figure 2.- Coordinate system and orbital orientation.

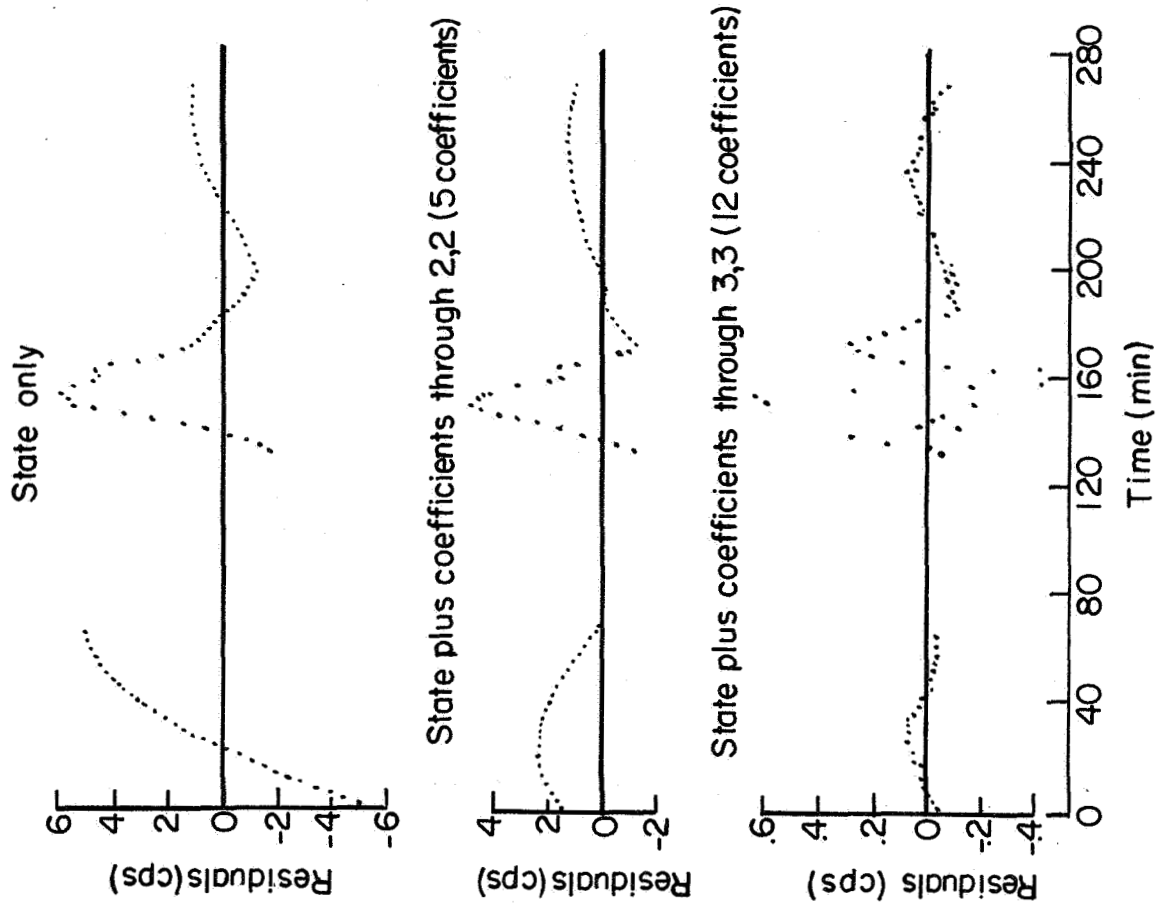


Figure 3.- Doppler residuals for different solution sets.

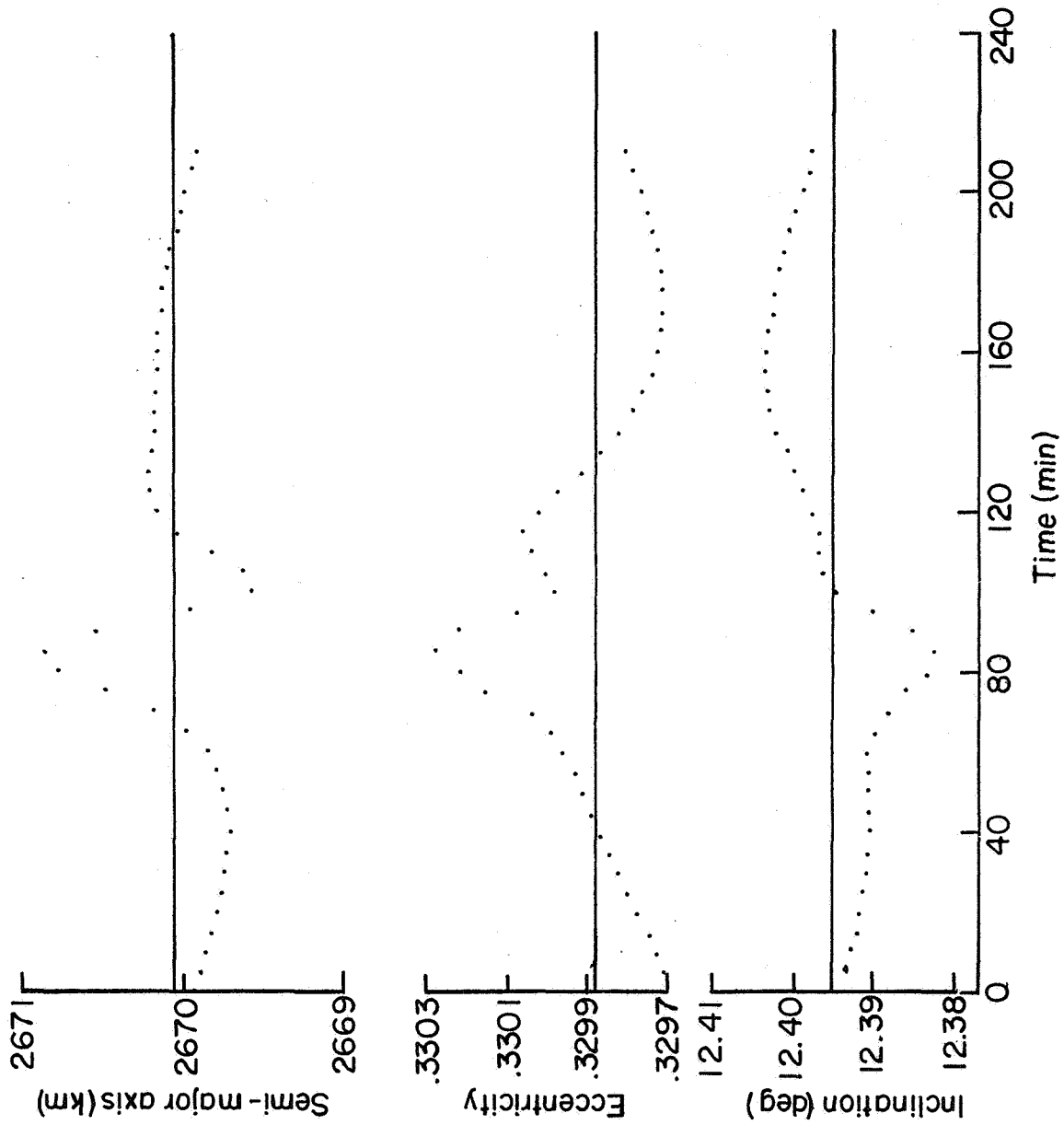


Figure 4.- Short-period variations in orbital elements.

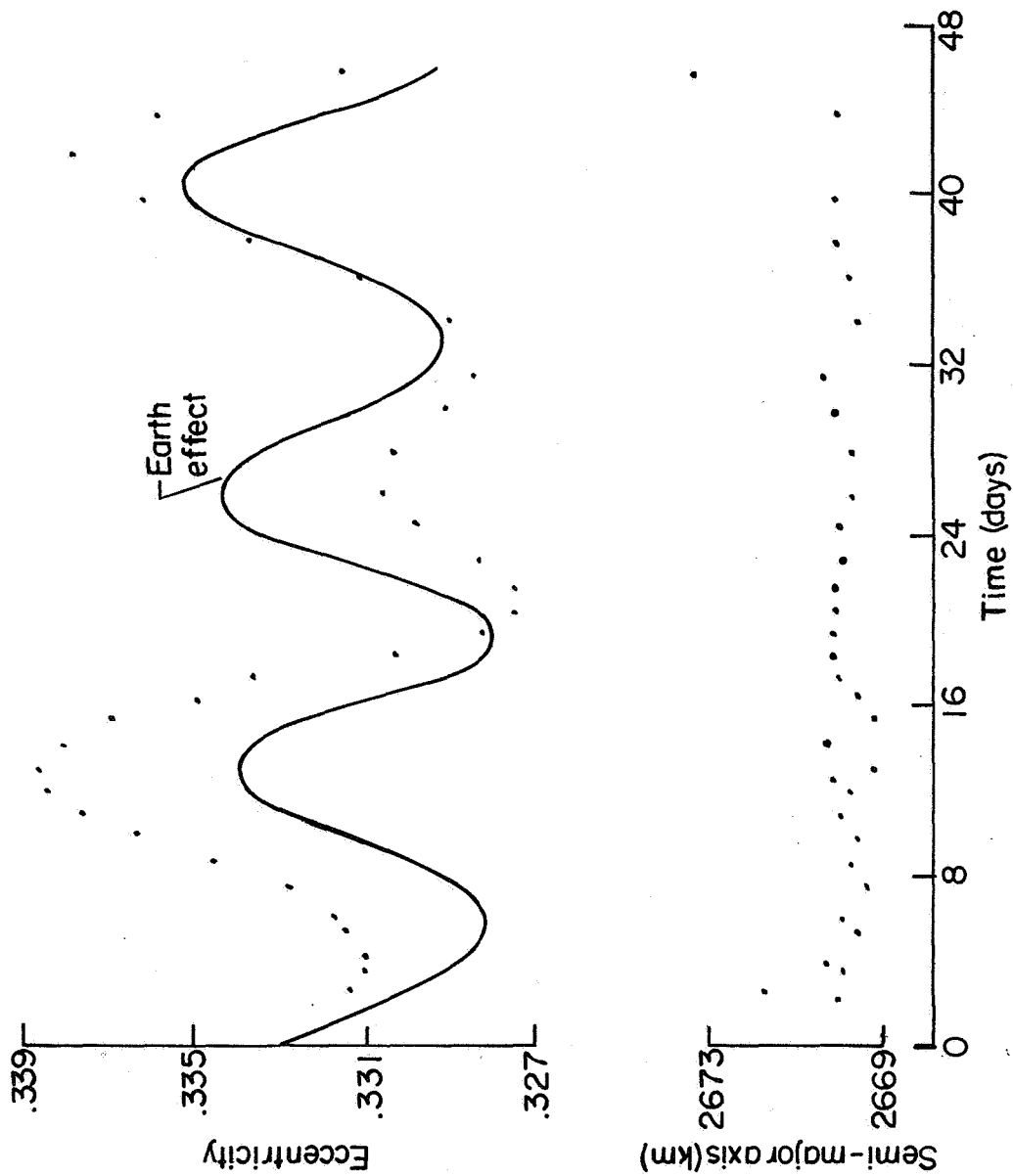


Figure 5a.- Long-period variations in orbital elements.

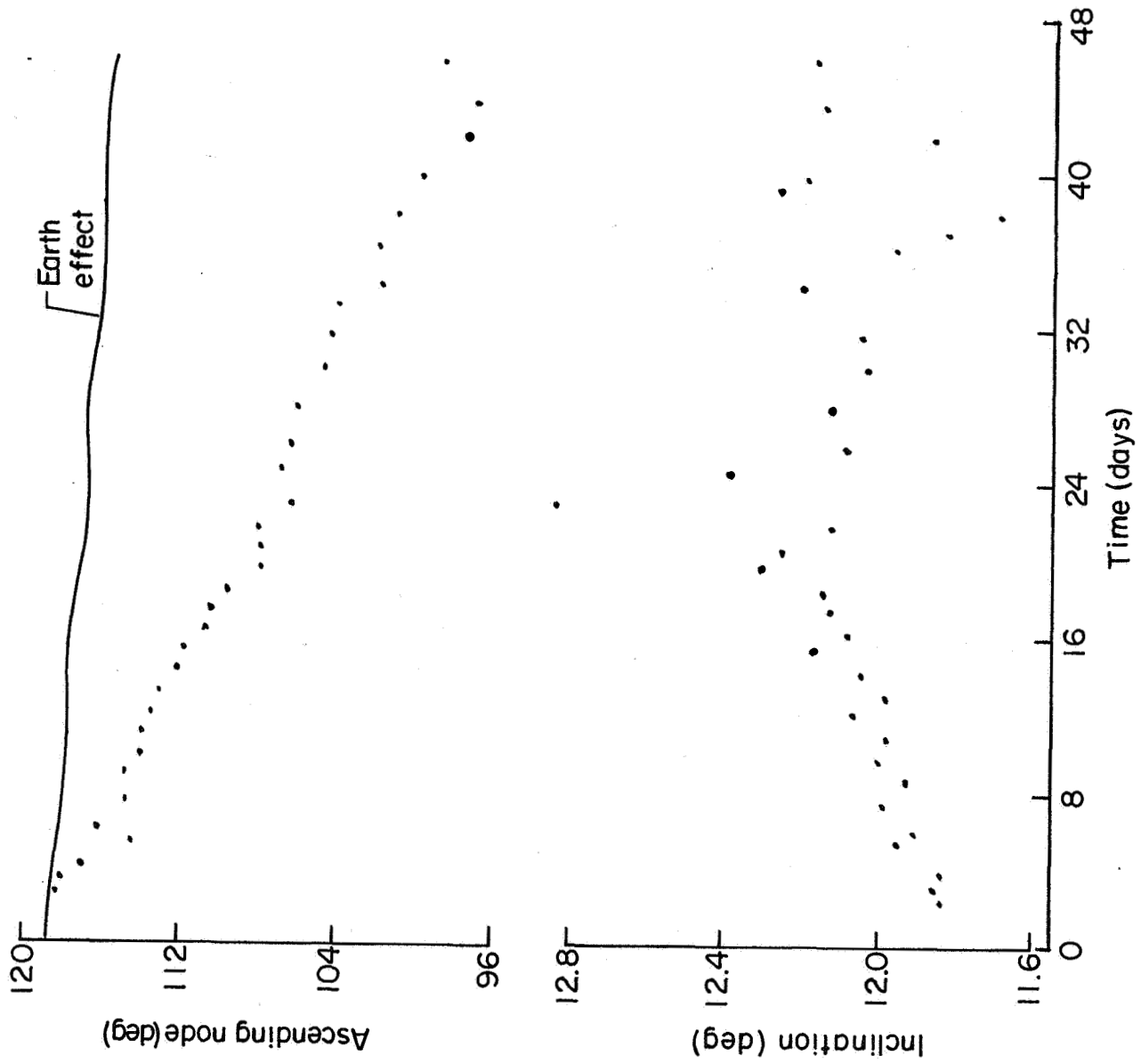


Figure 5b.- Long-period variations in orbital elements.

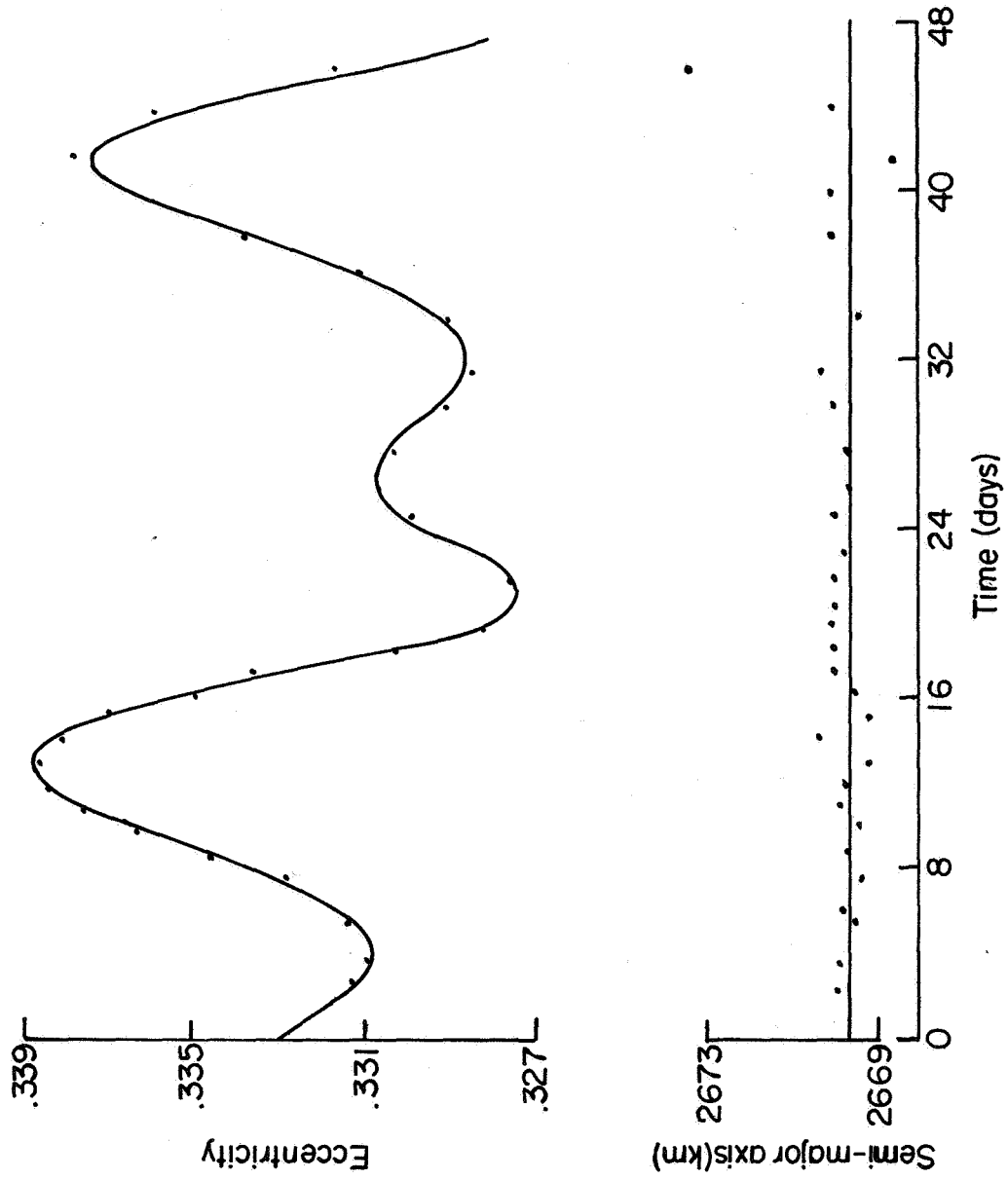


Figure 6a.- Data fit solving for state and coefficients through 3,3 plus 4,0.

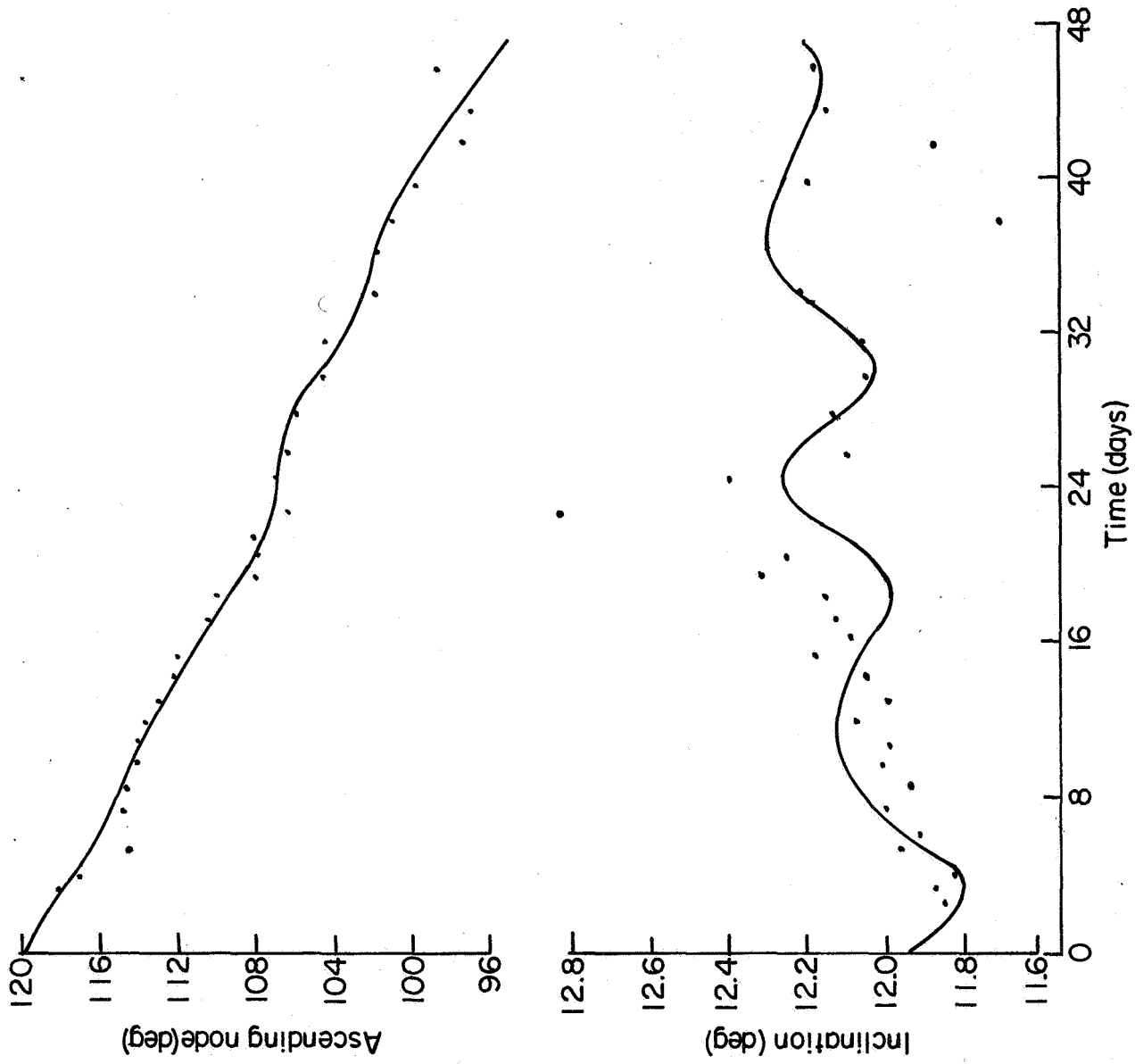


Figure 6b.- Data fit solving for state and coefficients through 3,3 plus 4,0.

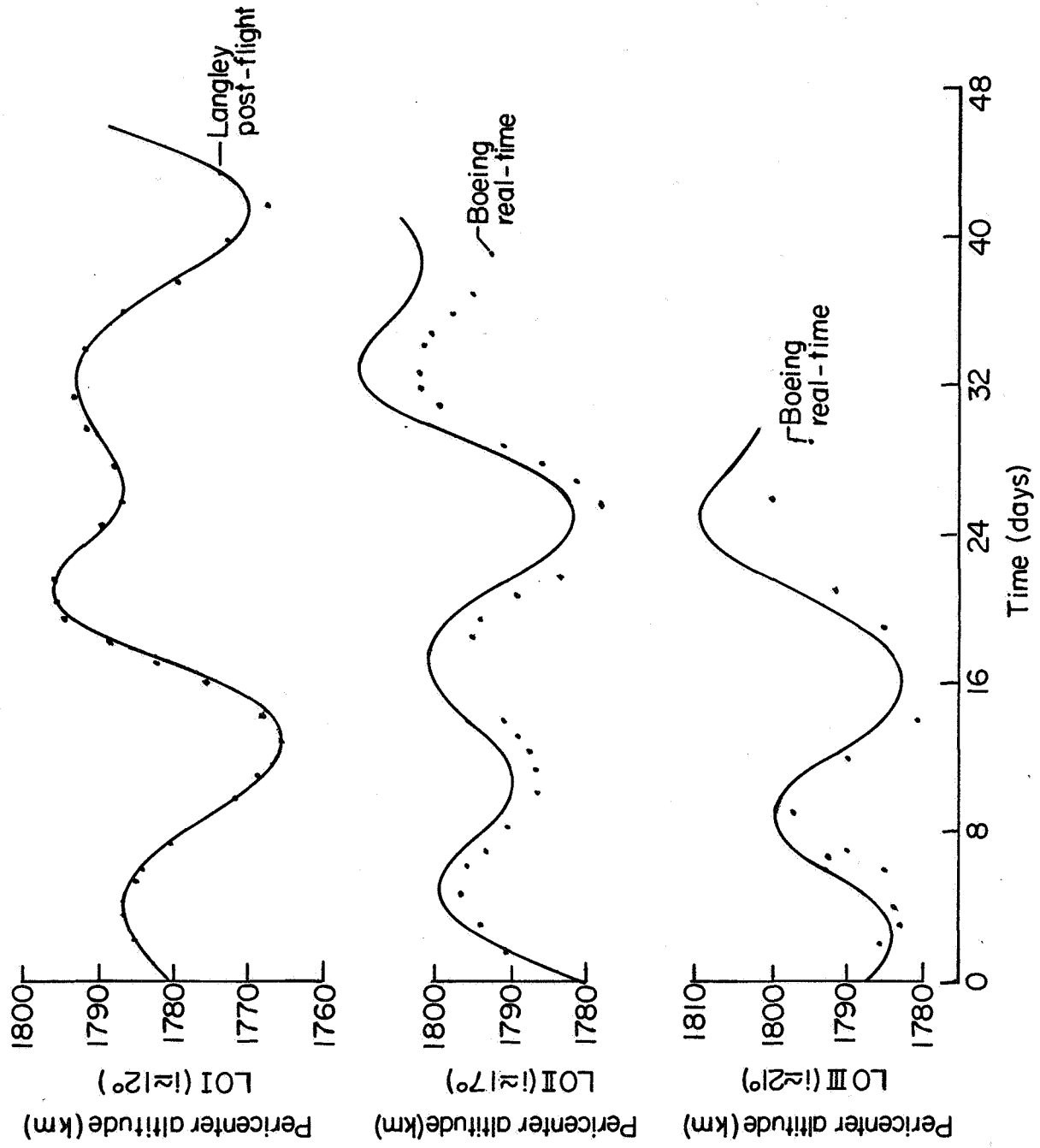


Figure 7.- Pericenter predictions for Lunar Orbiters I, II and III.

Table I

Preliminary lunar gravity field
from long - period analysis ($\times 10^4$)

$C_{2,0}$	-2.3691
$C_{3,0}$.3366
$C_{4,0}$	-.1368
$C_{2,1}$.0445
$S_{2,1}$	-.0363
$C_{2,2}$.2852
$S_{2,2}$.1027
$C_{3,1}$.3809
$S_{3,1}$.1115
$C_{3,2}$.0285
$S_{3,2}$.0064
$C_{3,3}$.1532
$S_{3,3}$.0537